

Ionoelectronics. Cation-Induced Nonlinear Complexation: Crown Ether- and Poly(ethylene oxide)-Substituted Lutetium Bisphthalocyanines

Thierry Toupance, Vefa Ahsen, and Jacques Simon*

Contribution from the ESPCI-CNRS, 10 rue Vauquelin, 75231 Paris cedex 05, France

Received January 11, 1994*

Abstract: Lutetium bisphthalocyanines symmetrically substituted with crown ether macrocycles ($[(15-C-5)_4Pc]_2Lu$, $[(18-C-6)_4Pc]_2Lu$) or linear poly(ethylene oxide) chains ($[(RO)_8Pc]_2Lu$) have been synthesized and characterized. An unsymmetrical complex ($[(15-C-5)_4Pc]Lu[Pc(OR)_8]$) is also described. The selectivity of complexation toward alkali cations is determined by the picrate extraction method. Titration curves have been obtained by UV-visible spectroscopy, showing that large alkali cations induce the formation of aggregates via a positive cooperativity effect. A sigmoidal titration curve is obtained for the couple $[(18-C-6)_4Pc]_2Lu/Rb^+$. The shape of the curve is very similar to the one obtained for the complexation of O_2 by hemoglobin, where a nonlinear binding process is well established. The obtainment of this phenomenon is a key step toward the realization of ionoelectronics networks.

Introduction

It has been reported that information processing at the molecular scale is on the verge of appearing in the domain of electronics. Molecules are used instead of inorganic materials but with the same function and, more importantly, with the same architecture of the circuits. Following this approach, connection problems arise which have not yet been satisfactorily solved even theoretically. A new way has been proposed^{1,2} in which the information is stored and treated by using ions (in particular alkali and alkaline earth cations). The term *ionoelectronics* has been proposed to name this field of research.^{1,2} It is noteworthy that ions are involved in most biological processes of information treatment. The use of ions for fabricating components has been mentioned.³ A schematic illustration of the architecture of the system we propose is shown in Figure 1.

A number of plugs (elementary complexing units) are functionalized with ligands. These ligands are designed in such a way that a *positive cooperative binding* can take place: the complexation of the first cation is more difficult than that of the second one. With this condition, it may be demonstrated that a nonlinear complexation of ions may occur, especially if some aggregation process characterized by a critical concentration (like in micelles) takes place (Figure 2).

Such a phenomenon occurs for the complexation of O_2 in the tetrameric subunits of hemoglobin. Positive cooperativity in ligands possessing several binding sites has also been described.⁴⁻⁶

The information is introduced within the system by addressing a certain number of elementary complexing units. This induces an ion diffusion between the plugs, leading to a switch of the units. A nonlinear complexation avoids a randomization of the information. The key step in this device is the design of a ligand able to yield a positive cooperative complexation.

For this purpose, four ligands have been designed (Figure 3), all of them based on the lutetium bisphthalocyanine subunit.

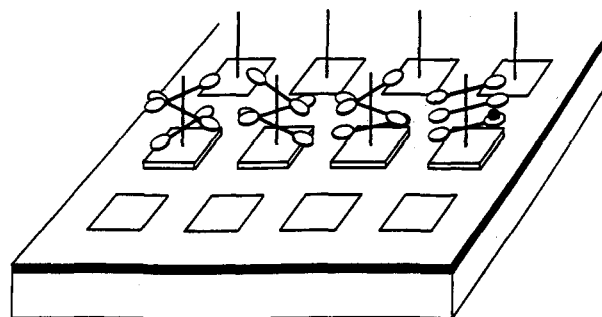


Figure 1. Schematic illustration of an ionoelectronics network based on a cooperative complexation on each elementary unit.

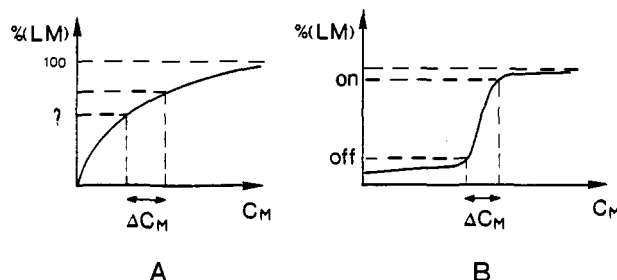


Figure 2. Proportion of complex LM as a function of the concentration of cation M. (A) Conventional complexation: $L + M \rightleftharpoons LM$. (B) Positive cooperativity effect: $L + M_1 \rightleftharpoons LM_1 (K_1)$; $LM_1 + M_2 \rightleftharpoons LM_1M_2 (K_2 > K_1)$. A critical concentration must be postulated to obtain a high nonlinearity, as shown in the figure.

Lutetium bisphthalocyanine (Pc_2Lu) is well known to form electrochromic thin films,^{7,8} and it is easily oxidized and reduced. This led to the demonstration of the intrinsic nature of the conductivity of this material.^{9,10} It was also possible to make field effect transistors with Pc_2Lu as active material.¹¹

* Abstract published in *Advance ACS Abstracts*, May 1, 1994.

(1) Le Berre, V.; Simon, J. *Molecular Materials for Electronics and Optoelectronics. Les Arcs* 1986, January.

(2) Simon, J.; Engel, M. K.; Soulié, C. *New J. Chem.* 1992, 16, 287.

(3) Lehn, J. M. In *Frontiers in Supramolecular Organic Chemistry*; Schneider, H. J., Durr, H., Eds.; VCH: Weinheim, 1991.

(4) Rebek, J., Jr.; Costello, T.; Marshall, L.; Wattlely, R.; Gadwood, R. C.; Onan, K. *J. Am. Chem. Soc.* 1985, 107, 7481.

(5) Tabushi, I.; Kugimiya, S.-I.; Kinnaird, M. G.; Sasaki, T. *J. Am. Chem. Soc.* 1985, 107, 4192.

(6) Pfeil, A.; Lehn, J. M. *J. Chem. Soc., Chem. Commun.* 1992, 838.

(7) Moskalev, P. N.; Kirin, I. S. *Russ. J. Phys. Chem.* 1972, 139, 335.

(8) Nicholson, M. M.; Pizzarello, F. A. *J. Electrochem. Soc.* 1979, 126, 1490.

(9) André, J. J.; Holczer, K.; Petit, P.; Riou, M. T.; Clarisse, C.; Even, R.; Fourmigué, M.; Simon, J. *Chem. Phys. Lett.* 1985, 115, 463.

(10) Turek, P.; Petit, P.; André, J. J.; Simon, J.; Even, R.; Boudjema, B.; Guillaud, G.; Maitrot, M. *J. Am. Chem. Soc.* 1987, 109, 5119.

(11) Guillaud, G.; Al Sadoun, M.; Maitrot, M.; Simon, J.; Bouvet, M. *Chem. Phys. Lett.* 1990, 167, 503.

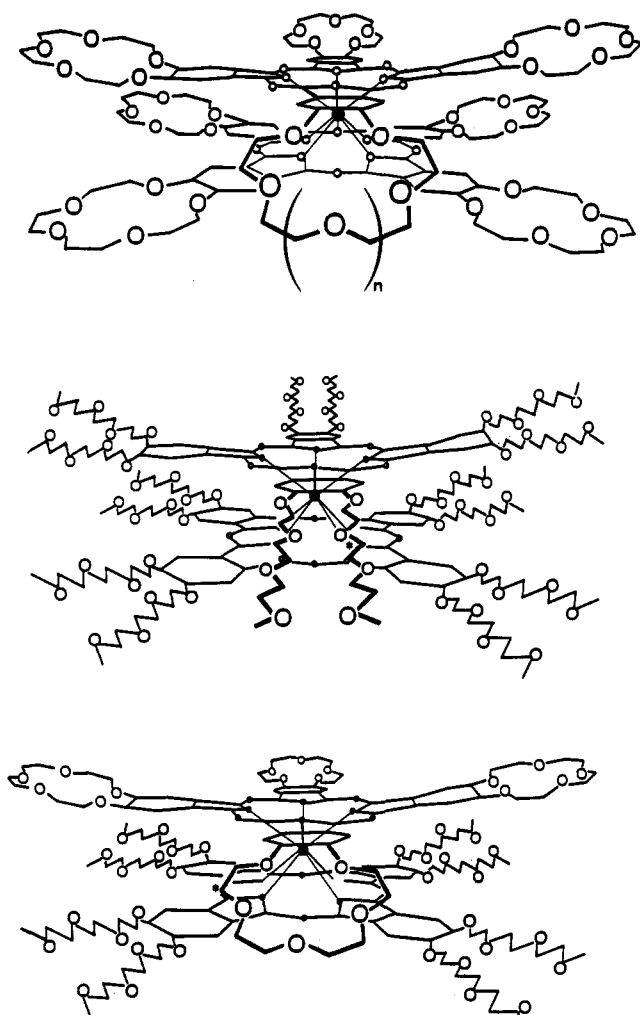


Figure 3. Representation of the ligands synthesized. Top, **1**, **2**: **1** [(15-C-5)₄Pc]₂Lu, *n* = 1; **2**, [(18-C-6)₄Pc]₂Lu, *n* = 2. Middle, **3**, [(RO)₈Pc]₂Lu. Bottom, **4**, [(15-C-5)₄Pc]Lu[Pc(OR)₈].

The substitution of single phthalocyanine rings with crown ether¹²⁻¹⁴ or poly(oxyethylene) side chains¹⁵ was already described. The size of the cavity available for the complexation has been varied (15-crown-5 or 18-crown-6 subunit) in order to discriminate different ions. Two types of complexation are expected to occur, depending on whether the ion can or cannot enter the crown ether cavity. In the latter case, sandwich complexes of two ligands and one cation are formed.

We report here the preparation of four new lutetium bisphthalocyanines¹⁶ **1-4** and their ¹H and ¹³C NMR characterizations. The ion complexation was studied by the conventional alkali picrate extraction method. The stoichiometry of complexation was determined by UV-visible absorption measurements.

Results and Discussion

Synthesis. The derivatives **1**, **2**, and **3** were synthesized from the corresponding substituted phthalonitriles by reaction with

(12) Sielcken, O. E.; Van Tilborg, M. M.; Roks, M. F. M.; Nolte, R. J. *M. J. Am. Chem. Soc.* **1987**, *109*, 4261.

(13) Kobayashi, N.; Lever, A. B. P. *J. Am. Chem. Soc.* **1987**, *109*, 7433.

(14) Ahsen, V.; Yilmazer, E.; Ertas, M.; Bekaroglu, O. *J. Chem. Soc., Dalton Trans.* **1988**, 401.

(15) Guillon, D.; Weber, P.; Skoulios, A.; Piechocki, C.; Simon, J. *Mol. Cryst. Liq. Cryst.* **1985**, *130*, 223.

(16) Part of this work has been described in a short communication: Toupance, T.; Ahsen, V.; Simon, J. *J. Chem. Soc., Chem. Commun.* **1994**, 75.

Lu(OAc)₃·3H₂O, 1,8-diazabicyclo[5.4.0]undec-7-ene (DBU), and hexan-1-ol^{17,18} (Scheme 1). Compounds **1** and **2** were purified by chromatography and recrystallization (CH₂Cl₂-*n*-pentane or *n*-heptane). Compound **3** could be reprecipitated from the same solvent mixture as a dark green paste. The overall yield is fairly low (5-20%) due to the numerous purification steps.

Several reports of unsymmetrically substituted lutetium bisphthalocyanines have been published in the literature.¹⁹⁻²⁵ Different synthetic routes have been proposed and involve the reaction between: (i) a lutetium monophthalocyanine and a phthalonitrile,¹⁹ (ii) a lutetium monophthalocyanine and a dihydrogenophthalocyanine,²⁵ (iii) two dilithiumphthalocyanines in the presence of a lutetium salt,^{22,23} and (iv) a lutetium monophthalocyanine and a dilithiumphthalocyanine.^{20,21,24} The last pathway leads to the highest yields.

The poly(oxyethylene)-substituted dilithium phthalocyanine was first tentatively synthesized. However, the reaction involves the use of pentanolate ions, which yield a transesterification of the poly(oxyethylene) side chains. The first method was then tried (Scheme 1): (15-C-5)₄PcLu(OAc)(2H₂O), synthesized according to the same procedure as was used for PcLuOAc,¹⁸ was reacted in hexan-1-ol in the presence of DBU with the phthalonitrile substituted with poly(oxyethylene) side chains. This latter compound was prepared in three steps, with an overall yield of 28% starting from commercially available pyrocatechol. The unsymmetrically substituted lutetium complex **4** was obtained in 7.5% yield. The final compound was separated from the two main side products, the poly(oxyethylene)-substituted dihydrogenophthalocyanine (*M*_w = 1812) and **1** (*M*_w = 2721), by preparative thin-layer chromatography.

NMR Studies. Only a few NMR data concerning lutetium bisphthalocyanine are available from the literature, most of them dealing with the reduced form.^{23,26,27} ¹H and ¹³C NMR studies have been carried out to characterize the various new products synthesized and also the adducts (stability constant, stoichiometry) form with alkali cations.

(i) **¹H NMR Spectroscopy.** The chemical shifts, assignments, and spectra in CDCl₃ of the neutral forms of **1-4** are given in detail in the Experimental Section. The assignments have been made by assuming that the protons closer to the aromatic ring are shifted toward low fields. The results are consistent for the four compounds studied. Aromatic and 2,2'-aliphatic protons (Table 1) are not observed distinctly in the neutral forms, probably because of their proximity to the paramagnetic center. However, a very broad signal around 5 ppm could be attributed to the 2,2'-hydrogen atoms. These results confirm that the paramagnetism of Pc₂Lu strongly perturbs the proton signals in the aromatic region, contrary to previously reported results.²⁶ The ¹H NMR spectrum of **4** clearly shows the unsymmetrical structure of the product (Figure 4): the four resonances at the highest fields are also found in compound **3**, whereas the two broad peaks at low field may be associated with protons present in both compounds **1** and **3** (see also Experimental Section). Integration values are consistent with this interpretation.

1 was reduced and oxidized to suppress molecular paramagnetism, and the corresponding NMR spectra were recorded.

(17) Tomoda, H.; Saito, S.; Ogawa, S.; Shiraishi, S. *Chem. Lett.* **1980**, 1277.

(18) De Cian, A.; Moussavi, M.; Fisher, J.; Weiss, R. *Inorg. Chem.* **1985**, *24*, 3162.

(19) Subbotin, N. B.; Tomilova, L. G.; Chernykh, E. V.; Kostromina, N. A.; Luk'yanets, E. A. *J. Gen. Chem. USSR* **1986**, *56*, 208.

(20) Liu, Y.; Shigehara, K.; Hara, M.; Yamada, A. *J. Am. Chem. Soc.* **1991**, *113*, 440.

(21) Ishikawa, N.; Ohno, O.; Kaizu, Y. *Chem. Phys. Lett.* **1991**, *180*, 51.

(22) Pondaven, A.; Cozien, Y.; L'Her, M. *New J. Chem.* **1991**, *15*, 515.

(23) Pondaven, A.; Cozien, Y.; L'Her, M. *New J. Chem.* **1992**, *16*, 711.

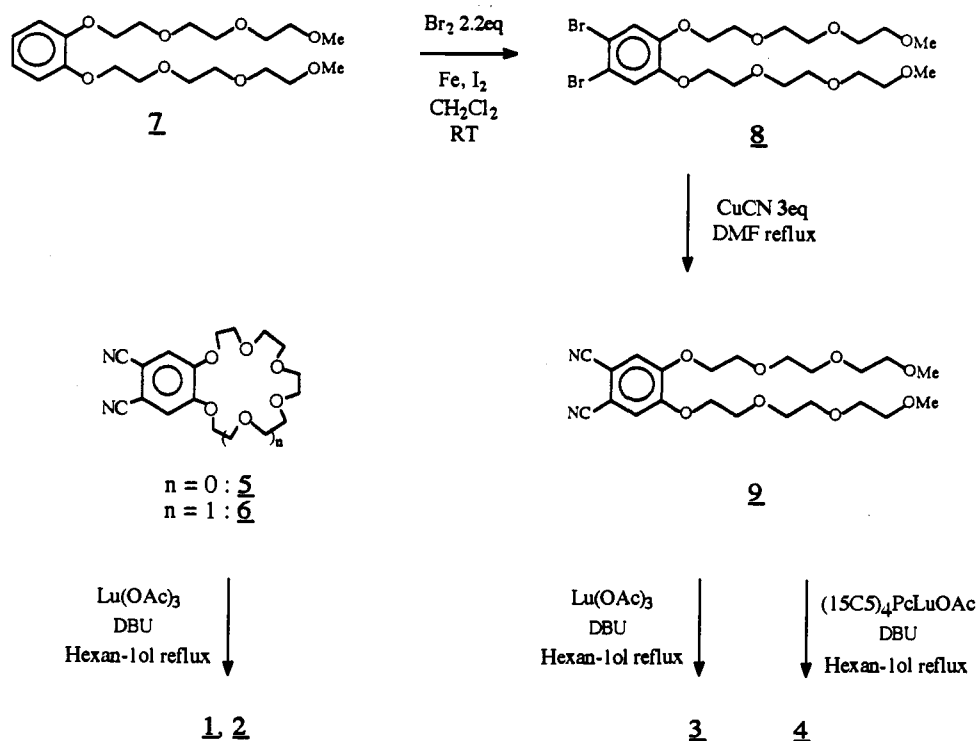
(24) Liu, Y.; Shigehara, K.; Yamada, A. *Bull. Chem. Soc. Jpn.* **1992**, *65*, 250.

(25) Ishikawa, N.; Kaizu, Y. *Chem. Phys. Lett.* **1993**, *203*, 472.

(26) Moussavi, M. Thèse de Doctorat, Université de Strasbourg, 1986.

(27) Konami, H.; Hatano, M.; Tajiri, A. *Chem. Phys. Lett.* **1989**, *160*, 163.

Scheme 1. Chemical Pathway Used To Synthesize the Complexes 1–4

Table 1. ^1H NMR Chemical Shifts (δ in ppm Downfield from TMS), Integration, and Assignments for Oxidized, Neutral, and Reduced Forms of 1

oxidized form ^a		neutral form ^b		reduced form ^c	
δ	atom	δ	atom	δ	atom
7.03 (16H)	1			8.50 (16H)	1
4.28 (16H)	2 or 2'			4.81 (16H)	2 or 2'
4.18 (16H)	2 or 2'			4.58 (16H)	2 or 2'
3.94 (32H)	3, 3'	4.10 (32H)	3, 3'	4.29 (16H)	3 or 3'
		3.99 (32H)	4, 4'	4.20 (16H)	3 or 3'
3.73 (64H)	4, 4', 5, 5'	3.89 (32H)	5, 5'	3.90 (64H)	4, 4', 5, 5'

^a CDCl_3 : CD_3OD 5:1. ^b CDCl_3 . ^c DMF.

Spectra data and assignments are given in Table 1. The assignments have been made by comparison with the corresponding 1,2-dicyanobenzocrown derivatives.^{12,14} (5: ^1H NMR δ 7.14 [2H, 1]; 4.19 [4H, 2, 2']; 3.91 [4H, 3, 3']; 3.73 [8H, 4, 4', 5, 5']. 6: ^1H NMR δ 7.16 [2H, 1]; 4.22 [4H, 2, 2']; 3.94 [4H, 3, 3']; 3.76 [4H, 4, 4']; 3.69 [4H, 5, 5']; 3.66 [4H, 6, 6'].)

Reduction has been carried out in $\text{DMF-}d_7$ with LiBH_4 . The alkali picrate extraction method (*vide infra*) showed that Li^+ is not complexed by 1 and 2 and, consequently, does not perturb the spectra.

In the spectrum of the reduced form, a peak in the aromatic region at 8.50 ppm is visible which is not present (or is extremely broad) in neutral 1. In the $-\text{OCH}_2-$ region, five different peaks are observed. The integration (32H) and the chemical shift permit the assignment of the 4 and 5 positions. This leaves four different

peaks for positions 2 and 3. The two halves of the crown ether macrocycles could be different by some distortion of the ring or some conformational effect. It is, however, more probable that the two protons on the same carbon atom are different and that outer and inner hydrogen atoms must be distinguished. In a staggered conformation, CPK models indicate that the methylene groups 2 and 3 overlap with the adjacent subunit. This leads to the differentiation of the hydrogen atoms depending on whether they are turned toward or out from the interphthalocyanine space.

H–H decoupling experiments show that the peaks at lowest field (2,2' and 3,3') are coupled together. This is in agreement with our previous hypothesis.

Oxidation of 1 was carried out with bromine in a CDCl_3 : CD_3OD mixture. In the aromatic region, a peak at 7.03 ppm is detected, significantly shifted compared to that of the reduced form (8.50 ppm).

(ii) ^{13}C NMR Spectroscopy. Spectral data and assignments for 1 are gathered in Table 2 (see also Experimental Section). Benzo-18-crown-6 was used as a reference for the C-atoms in the ether region.^{28,29} The peaks in the aromatic region were assigned by using a conventional additivity law and the results previously found for $(15\text{-C-}5)_4\text{PcPb}$.³⁰

The carbon atoms close to the central aromatic core are not observed in the neutral forms. Oxidation and reduction restore the expected resonances.

The NMR results indicate a diamagnetic state of the oxidized form; this is, however, not entirely consistent with the disappearance of the intermacrocyclic charge-transfer band around 1400 nm in the optical absorption spectrum of the oxidized lutetium complex (*vide infra*).

Complexation properties of 1 toward alkali ions (Li^+ , Na^+ , K^+) have been investigated. No change in the ^{13}C spectrum is observed on addition of LiSCN to a solution of 1; this indicates a weak complexation of Li^+ by the crown ether subunits. Addition of K^+ leads, on the contrary, to precipitation. Addition of small

(28) Fedarko, M. C. *J. Magn. Reson.* 1973, 12, 30.

(29) Live, D.; Chan, S. I. *J. Am. Chem. Soc.* 1976, 98, 3775.

(30) Ahsen, V.; Yilmazer, E.; Gürek, A.; Gül, A.; Bekároglu, Ö. *Helv. Chim. Acta* 1988, 71, 1616.

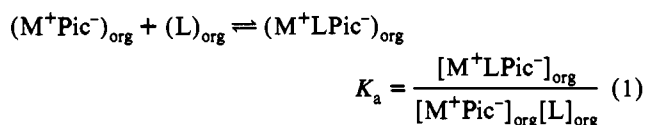
portions of NaSCN in methanol yields important changes in the NMR spectra up to a $\text{Na}^+ : 1$ ratio of 8:1. Further addition does not modify the spectrum, indicating that eight Na^+ are complexed within each molecular unit. The exchange rate of the cations between the occupied and metal-free crown ether sites is fast at the NMR time scale ($\nu_{\text{ex}} \gg 570 \text{ s}^{-1}$).

Ion Complexation: $\text{H}_2\text{O}/\text{CHCl}_3$ Extraction Method. A conventional $\text{H}_2\text{O}/\text{CHCl}_3$ extraction method has been used to determine the binding constant of the ligands with the alkali cations.³¹⁻³³ In this technique, a picrate salt is dissolved in water, and the ligand (presumed to be hydrophobic) is in the chloroformic phase. At equilibrium, a certain amount of picrate salt is extracted; this amount (R) is related to the stability constant of the cation/ligand:

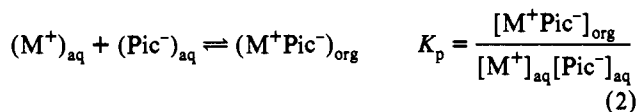
$$R = \frac{[\text{M}^+\text{Pic}^-]_{\text{ex}}}{[\text{L}_0]}$$

with $[\text{M}^+\text{Pic}^-]_{\text{ex}}$ being the concentration of salt extracted in CHCl_3 and $[\text{L}_0]$ the initial concentration of ligand.

In the case of the stoichiometry of complexation being 1:1, the corresponding association constant can be obtained:



To calculate K_a , it is necessary to take into account the solubility of the picrate salt in CHCl_3 in the absence of ligand:³²



It is then possible (See Experimental Section) to calculate K_a and the corresponding free enthalpy of complexation. It is, however, worth pointing out that the absolute values of K_a are difficult to obtain in this way since, in particular, the amount of water extracted together with the cation depends on the nature of the cation. In the following discussion, only qualitative features will be retained.

If the ligand possesses several binding units, the initial concentration in binding sites $[\text{CR}_0]$ is substituted for $[\text{L}_0]$. In our case, $[\text{CR}_0] = 8[\text{L}_0]$. The independence of the binding sites is assumed at that stage.

For cations bigger than the internal crown ether cavity (K^+ , Rb^+ for **1**, and Rb^+ , Cs^+ for **2**), the stoichiometry of complexation is not known with certainty (*vide infra*), and the association constant cannot be rigorously calculated: only the extracted ratio parameter R is relevant in this case (Table 3).

Na^+ and K^+ form the most stable complexes with **1** and **2**, respectively. This is the expected selectivity.³⁴ **2** leads to more stable complexes than **1** for the optimum size cations. This is consistent with the reported data on the thermodynamics of complexation of benzocrown derivatives: the stability constants of benzo-18-crown-6 derivatives are always higher than those of derivatives possessing benzo-15-crown-5 moieties.^{34,35}

The extraction determinations have been made as a function of the concentration of ligand in the case of **1**: significant

(31) Moore, S. S.; Tarnowski, T. L.; Newcomb, M.; Cram, D. J. *J. Am. Chem. Soc.* **1977**, *99*, 6398.

(32) Koenig, K. E.; Lein, G. M.; Stuckler, P.; Kaneda, T.; Cram, D. J. *J. Am. Chem. Soc.* **1979**, *101*, 3553.

(33) Helgeson, R. C.; Wiesman, G. R.; Toner, J. L.; Tarnowski, T. L.; Chao, Y.; Mayer, J. M.; Cram, D. J. *J. Am. Chem. Soc.* **1979**, *101*, 4928.

(34) Izatt, R. M.; Pawlack, K.; Bradshaw, J. S.; Bruening, R. L. *Chem. Rev.* **1991**, *91*, 1721.

(35) Dietrich, B.; Viout, P.; Lehn, J. M. *Aspects de la chimie des composés macrocycliques*; Interditions/éditions du CNRS: Paris, 1991; pp 338-342.

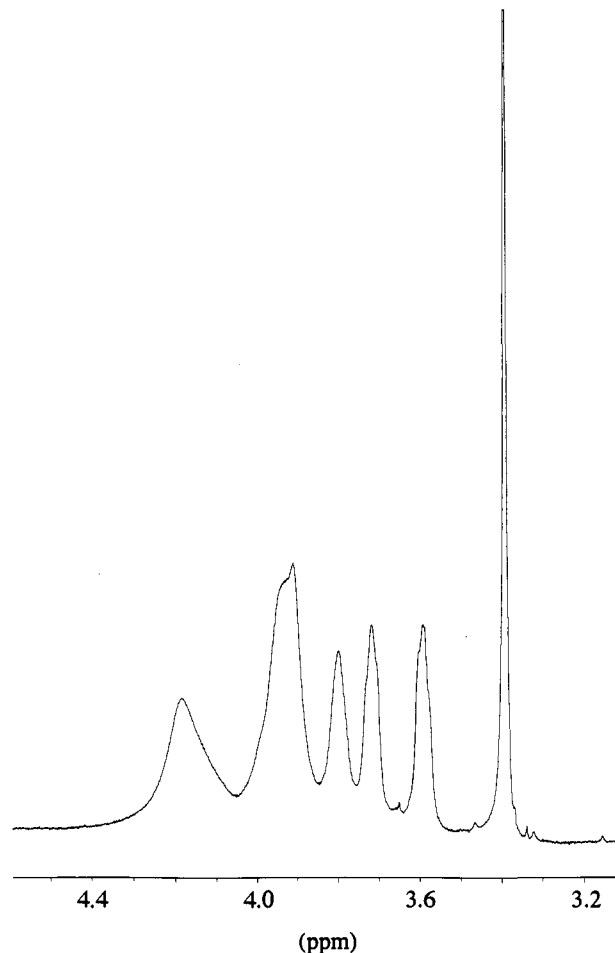


Figure 4. ^1H NMR spectrum of the unsymmetrical ligand **4**.

Table 2. ^{13}C NMR Chemical Shifts (δ in ppm Downfield from TMS) and Assignments for Oxidized, Neutral, and Reduced Forms of **1**

oxidized form ^a		neutral form ^b		reduced form ^a	
δ	atom	δ	atom	δ	atom
164.3	1			158.9	1
153.3	4			149.9	4
132.6	2			131.7	2
108.0	3			105.7	3
70.8	8	70.8	8	70.2	8
70.2	7	70.0	7	69.6	7
70.0	6	69.3	6	69.0	6
69.5	5			68.8	5

^a $\text{CDCl}_3/\text{CD}_3\text{OD}$ 5:1. ^b CDCl_3 .

deviations from the values shown in Table 3 have been found ($[\text{CR}_0] = 3 \times 10^{-3} \text{ M}$; $10^{-5} K_a$ in M^{-1} : Li^+ , 1.1; Na^+ , 8.8; K^+ , (3.2); Rb^+ , (0.5)). A decrease of the Na^+/K^+ selectivity as $[\text{CR}_0]$ increases is observed. The formation of aggregates at high ligand concentrations is probably responsible for this effect.

Electrochemistry of $[(15\text{-C-5})_4\text{Pc}]_2\text{Lu}$. Chloroformic solutions of **1** have been studied by UV-visible absorption spectrometry. The spectrum of the neutral form is very similar to the one observed for unsubstituted Pc_2Lu^7 (Table 4). **1** is oxidized to the red form with dichlorodicyanoquinone, whereas N_2H_4 yields the reduced

Table 3. Complexation Properties of **1** and **2** (Picrate Extraction Method)^a

	1			2		
	<i>R</i> (%)	10 ⁻⁵ <i>K</i> _a (M ⁻¹)	-Δ <i>G</i> ₀ (kJ/mol)	<i>R</i> (%)	10 ⁻⁵ <i>K</i> _a (M ⁻¹)	-Δ <i>G</i> ₀ (kJ/mol)
Li ⁺	0.32	0.9	28.2	0.42	1.2	28.9
Na ⁺	3.16	8.0	33.7	1.54	3.7	31.8
K ⁺	3.13	(5.4)	(32.7)	34.5	192.5	41.6
Rb ⁺	0.45	(0.4)	(26.8)	20.5	(35.6)	(37.4)
Cs ⁺	ε			6.9	(6.3)	(33.1)

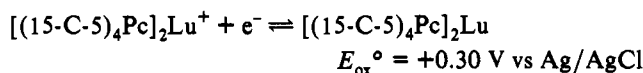
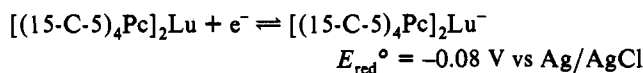
^a *R*, extracted ratio; *K*_a, association constant; Δ*G*₀, free enthalpy of complexation at 25 °C, [M₀] = 5 × 10⁻³ M, [CR₀] = 5 × 10⁻³ M. Values are given in parentheses when the stoichiometry of complexation is not known with certainty.

Table 4. Absorption Characteristics of the Neutral, Reduced, and Oxidized Forms of **1** in CHCl₃

oxidized form		neutral form		reduced form	
λ (nm)	10 ⁻⁵ ε (M ⁻¹ cm ⁻¹)	λ (nm)	10 ⁻⁵ ε (M ⁻¹ cm ⁻¹)	λ (nm)	10 ⁻⁵ ε (M ⁻¹ cm ⁻¹)
291		290	(1.0)	284	
385	(1.2)	367	(1.3)	366	(1.6)
498	(0.8)	476	(0.4)		
		602	(0.3)	626	(1.6)
703	(0.5)	666	(1.6)	705	(0.6)
940	(0.32)	910	(0.06)		
		1280	(s)		
		1390	(0.16)		
		1500	(s)		

blue form. The intramolecular charge-transfer band at λ_{max} = 1390 nm disappears by reduction and by oxidation as with Pc₂-Lu.³⁶

[(15-C-5)₄Pc]₂Lu can be easily deposited by spin coating on semitransparent SnO₂ electrodes. The redox properties of the thin films may then be determined by cyclic voltammetry:³⁷



Redox cyclings were repeated without noticeable degradation of the films. A mirage effect³⁸ has been used to detect the ion movements arising at the interface between the organic layer and the aqueous medium.

When a negative voltage is applied, **1** is reduced, and a laser beam deviation corresponding to the entrance of a cation is observed (Figure 5). The ratio of the mirage deviation over the electrochemical current (θ/*i*) permits the estimation³⁹ that there is approximately one cation complexed per reduced form of **1**. This stoichiometry ensures the electroneutrality.

It is therefore possible to couple the reduction of the central phthalocyanine core with a cation binding process in the crown ether macrocycles. This can be used later to address an elementary unit by electrical means.

Nonlinear Complexation of Cations. The complexation of alkali cations has been studied by UV-visible absorption spectroscopy. By addition of a picrate salt (dissolved in methanol) to a

(36) Markovitsi, D.; Tran-Thi, T. H.; Even, R.; Simon, J. *Chem. Phys. Lett.* **1987**, *137*, 107.

(37) Bardin, M.; Bertounesque, E.; Plichon, V.; Simon, J.; Ahsen, V.; Bekaroglu Ö. *J. Electroanal. Chem.* **1989**, *271*, 173.

(38) Russo, R. E.; McLarnon, F. R.; Spear, J. D.; Cairns, E. J. *J. Electrochem. Soc.* **1987**, *134*, 2783.

(39) When, one ion enters the film, it has been shown that the ratio θ/*i* is a constant for a given electrolyte when the geometry of the electrode and the transport characteristics of the electrolyte are known. Thus, θ/*i* is equal to 2.5 rad·cm⁻¹·A⁻¹ for KCl, the electrolyte which was used. If *n* cations enter the film, this value will be multiplied by *n*. Plichon, V., private communication.

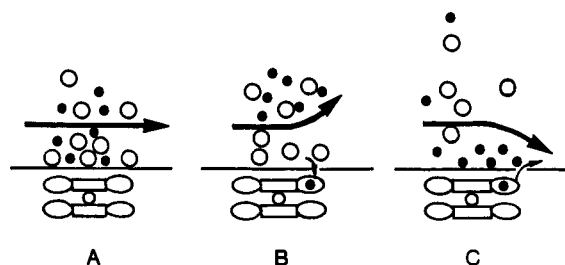


Figure 5. Deviation of a laser beam by the complexation or decomplexation of potassium ion in thin films of **1**. (A) Steady-state: the neutral complex does not bind the cation. (B) Reduction: the cation enters the crown ether cavity, and a depletion layer is generated at the interface. (C) Reoxidation: decomplexation occurs, increasing the concentration of cation at the interface.

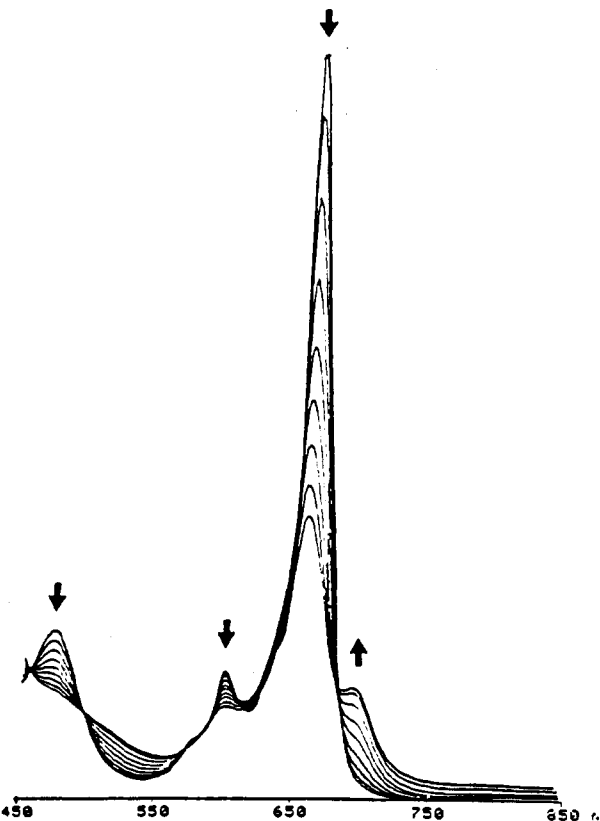


Figure 6. Absorption spectrum of **1** (Q-band) in CHCl₃ as a function of the concentration of potassium picrate. Arrows indicate the direction of the spectroscopic changes. The final spectrum corresponds to a solution saturated with potassium picrate.

chloroformic solution of ligands, the absorbance of the Q-band (666 nm) of **1**, **2**, and **4** is changed (Figure 6).

The presence of isosbestic points indicates that definite species are formed. The decrease of the absorbance strongly depends on the nature of the cation.

Na⁺ has been previously shown to form the most stable complexes with **1** by the picrate extraction method. However, the addition of sodium picrate to a chloroformic solution of **1** does not significantly modify its absorption spectrum. Li⁺, which is not complexed, also leads to small modifications. Intracavity complexation is therefore not the cause of the absorbance changes observed. On the contrary, K⁺ and Rb⁺ have pronounced effects: these cations are both too large to be accommodated within the internal cavity of the crown ether moieties (Figure 7).

Dimerization^{12,13} and oligomerization^{40,41} are known to shift and broaden the Q-band of phthalocyanine subunits. A similar

(40) Kane, A. R.; Sullivan, J. F.; Kenney, D. H. *Inorg. Chem.* **1970**, *9*, 1445.

(41) Sirlin, C.; Bosio, L.; Simon, J. *Mol. Cryst. Liq. Cryst.* **1988**, *155*, 231.

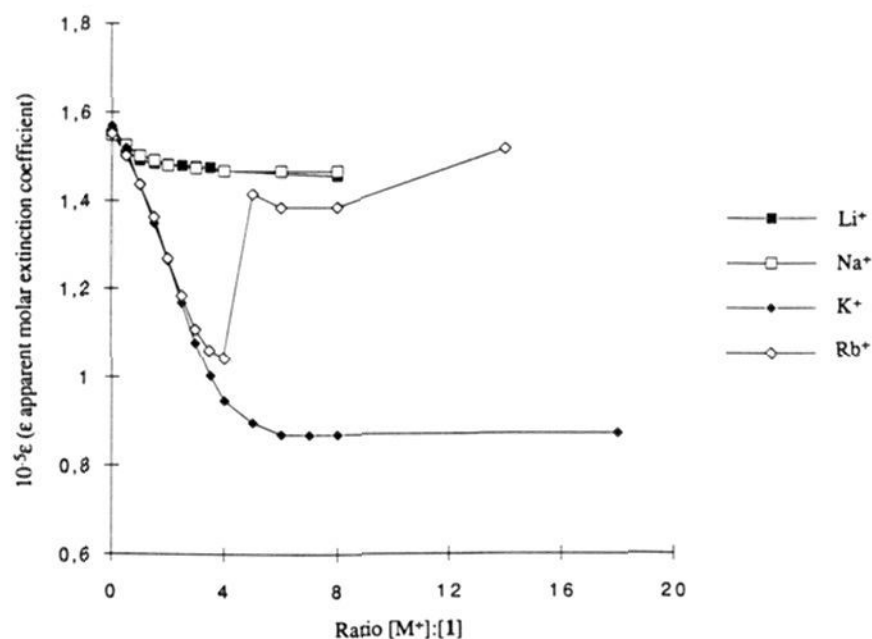


Figure 7. Apparent molar extinction coefficient, ϵ , of the Q-band of **1** as a function of the concentration of picrate salts. (For the definition of ϵ , see Experimental Section.)

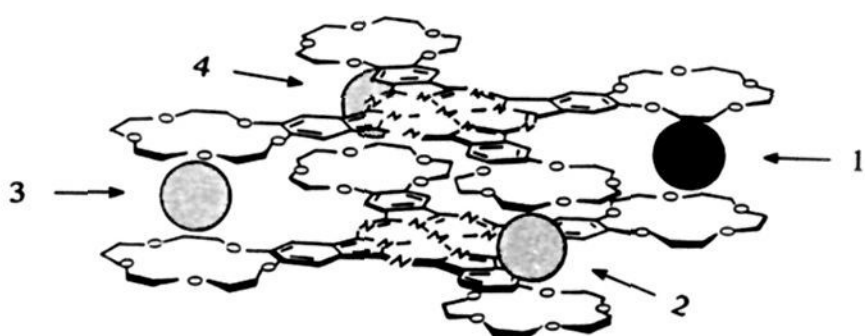


Figure 8. Schematic representation of the cooperative complexation of cations in a dimeric system. Preorganization is achieved by the cation number 1, facilitating the binding of the three other cations (redrawn from ref 13).

phenomenon is therefore expected to arise for ligand **1**. In the case of (15-C-5)₄PcCu and (18-C-6)₄PcCu, the decrease of the absorbance of the Q-band as a function of the concentration of the cation¹² is approximately a straight line from the origin to a plateau value corresponding to a stoichiometry of 2:1 (four cations:two ligands). A sandwich dimer has been postulated to rationalize these results.^{12,13} The slope of the titration curve being constant until all the binding sites are occupied, it is highly probable that a positive cooperative mechanism takes place (Figure 8).

In the first step, a cation forms a sandwich complex with two crown ether phthalocyanine ligands. The stability constant of this first equilibrium is relatively low. In a second step, the second, third, and fourth cations are complexed with a larger complexation constant due to a proper organization of the crown ether macrocycles. The addition of the three extra cations does not modify the concentration of the sandwich complex and does not consequently affect the absorbance of the Q-band. In the case of ligand **1**, the same type of titration curve is observed (Figure 9b), but the addition of salts influences the absorption spectrum up to a ratio of four M⁺ per ligand when M⁺ = K⁺ or Rb⁺.

The ligand **1** possesses two sets of four crown ether-substituted phthalocyanine groups linked by a lutetium(III) ion. If sandwich complexes are formed with both sets, one-dimensional aggregates must be formed (Figure 10).

Two different routes are possible toward high molecular weight aggregates, depending on the stoichiometry of the ion binding complexation at each stage of the sandwich complex formation.

In the limit $K_1 \gg K_i$ ($i > 1$), aggregates are formed with a stoichiometry of one cation per ligand. Since only aggregation leads to detectable absorption changes, no further modification of the spectrum is expected. This is not in agreement with the experimental titration curve of ligand **1**, where a 4:1 stoichiometry is reached. As for the substituted monophthalocyanines, a positive

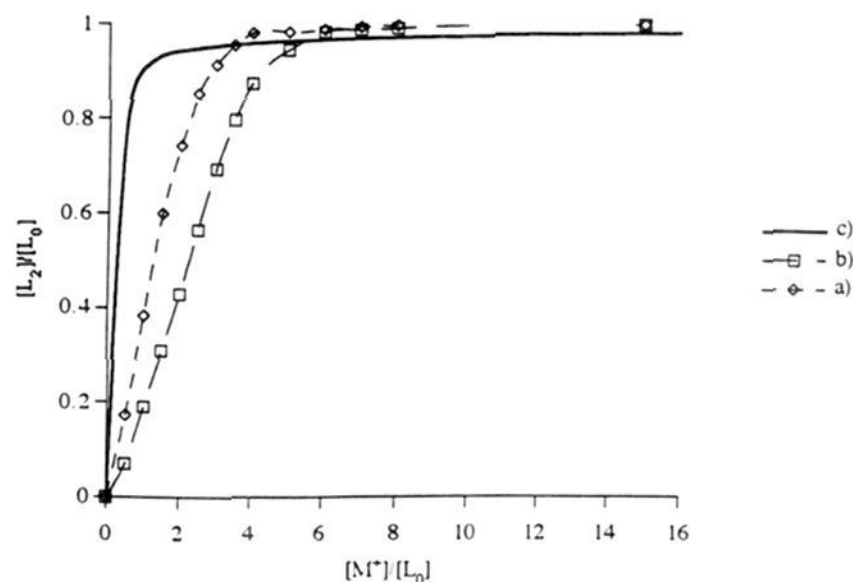


Figure 9. Proportion of ligand **1** in some aggregated form as a function of the ratio cation:ligand **1** (solvent CHCl₃). Experimental titration curves: (a) K⁺:ligand **4**; (b) K⁺:ligand **1**. (c) Calculated curve for the equilibrium $2L + M \rightleftharpoons L_2M$ ($K = 10^{12}$).

cooperative effect must be postulated. The formation of a new sandwich complex does not take place before all the crown ether binding sites of the aggregate are filled with cations. At each stage of the formation of the aggregate, $K_1 < K_2, K_3, K_4$ (Figure 10). The increase of the stability constant brought by the preorganization of the crown ether macrocycles prior to complexation may be estimated:⁴² an enhancement of the order of 100 is expected.

When the four binding sites have been filled, a new floor can be built by complexing four new cations, leading finally to high molecular weight columnar aggregates. The aggregation number N must be sufficiently large ($N > 20$) to give the experimental ratio of four cations per ligand.

The two cations K⁺ and Rb⁺ lead to the same type of curve up to the stoichiometry four cations per ligand. The same aggregation process therefore takes place. However, aggregates seem to be disrupted at high concentrations in Rb⁺: this indicates that the formation of complexes with stoichiometries higher than 4:1 is possible in this case.

The same studies have been carried out for the unsymmetrical lutetium complex **4** (Figure 9a). For the complexation of the potassium ion, a plateau value corresponding to a stoichiometry 2K⁺:**4** is obtained. The poly(oxyethylene) chains are very weak cation complexing subunits, and they are not expected to yield sandwich-type complexes. The aggregation stops at the dimeric stage. A similar behavior was recently reported for the unsymmetrical compound [Pc]Lu[15-C-5)₄Pc].²⁵ Compound **3** without crown ether subunits shows no significant spectral change by addition of cations.

Compound **2** has been studied with the same methods. The most easily bound cation, K⁺, does not lead to any significant spectral change. Cs⁺ leads to a titration curve very similar to the one previously observed for the couple **1**-K⁺. On the contrary, Rb⁺ yields a sigmoidal curve (Figure 11).

The shape of the curve indicates that the formation of aggregates is difficult at low cation concentration and is facilitated beyond a certain threshold. This behavior is analogous to that observed for hemoglobin, where there is a positive cooperativity effect for the binding of O₂ (Figure 11e). In myoglobin, where intersite cooperativity is impossible, the titration curve exhibits the conventional shape (Figure 11d).

Compound **2** in the presence of Rb⁺ leads to two different nonlinear complexation processes. The cooperative cation complexations occurring at each stage of the formation of aggregates are probably identical to each previous one. However, besides

(42) Simon, J.; Le Moigne, J.; Markovitsi, D.; Dayantis, J. *J. Am. Chem. Soc.* **1980**, *102*, 7247.

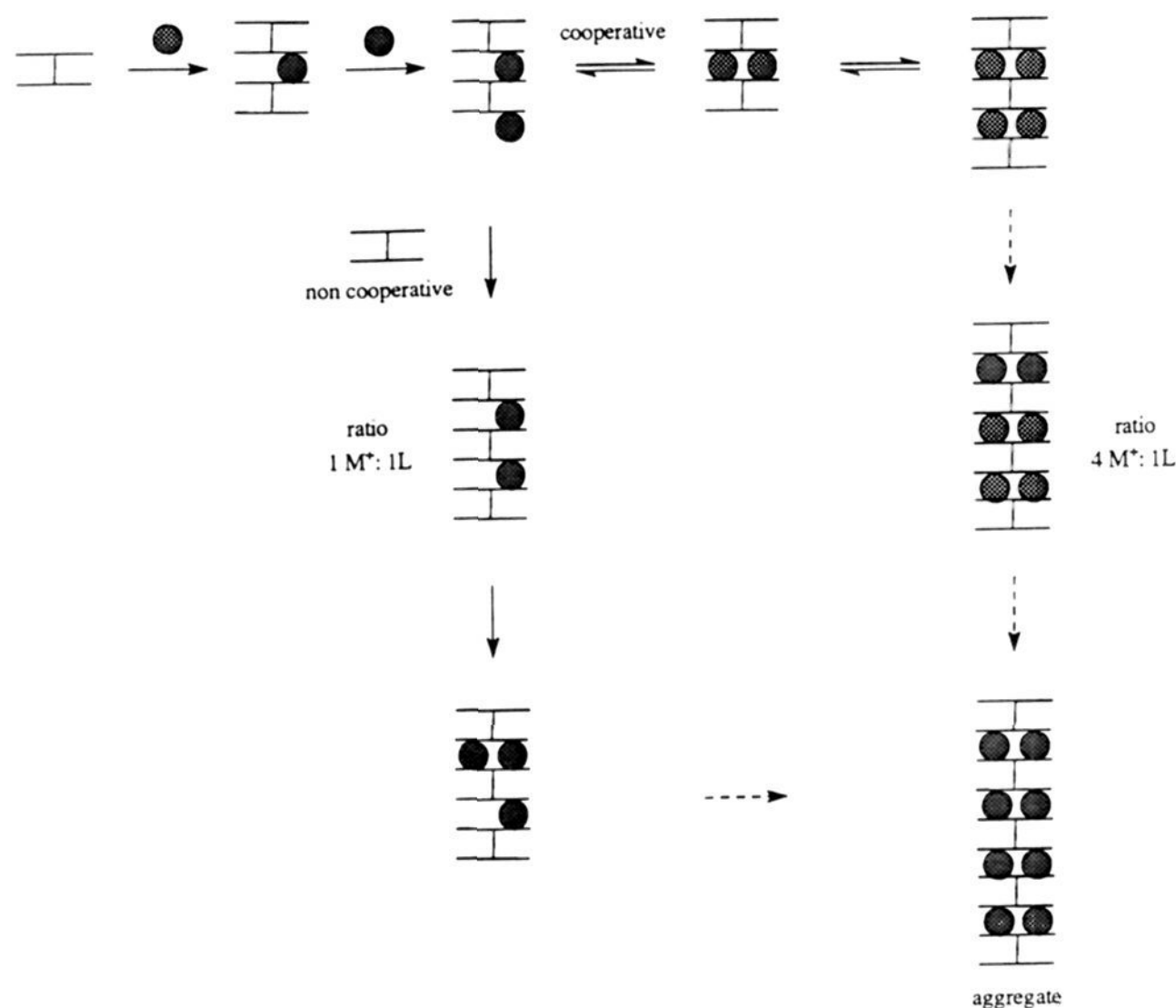


Figure 10. Schematic representation of the cooperative and noncooperative binding processes which can be observed for the complexation of cations with **1** (only four binding sites per molecular unit have been figured for clarity reasons).

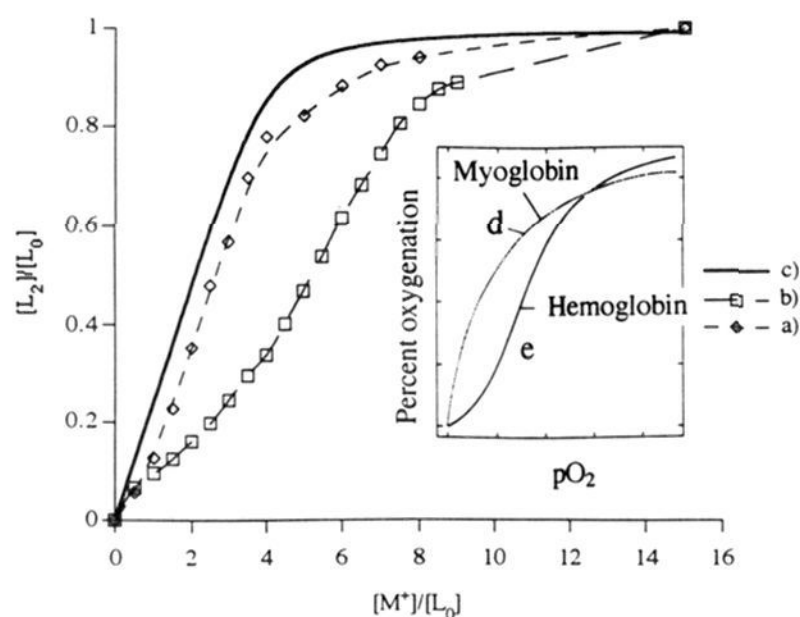


Figure 11. Titration curves showing the proportion of ligand **2** in an aggregated form versus the ratio $M^+:2$ (solvent: CHCl_3). (a) Cs^+ , (b) Rb^+ . (c) Calculated for $L + M \rightleftharpoons LM$ ($K = 10^6$; $L'_0 = 4L_0$). For comparison, the curves corresponding to the complexation of O_2 by myoglobin (d) and hemoglobin (e) have been represented in the inset.

this phenomenon, it seems that aggregates cannot be found below a given critical concentration (Figure 12).

The formation of micelles, for instance, also occurs above a critical concentration; the same kind of cooperativity must be considered in our case.

Calculations have been carried out confirming that the two cooperativity effects must be simultaneously present for rationalizing the sigmoidal shape of the titration curve shown in Figure 11.

Conclusion

New lutetium bisphthalocyanine complexes substituted with crown ether macrocycles have been synthesized. The coupling

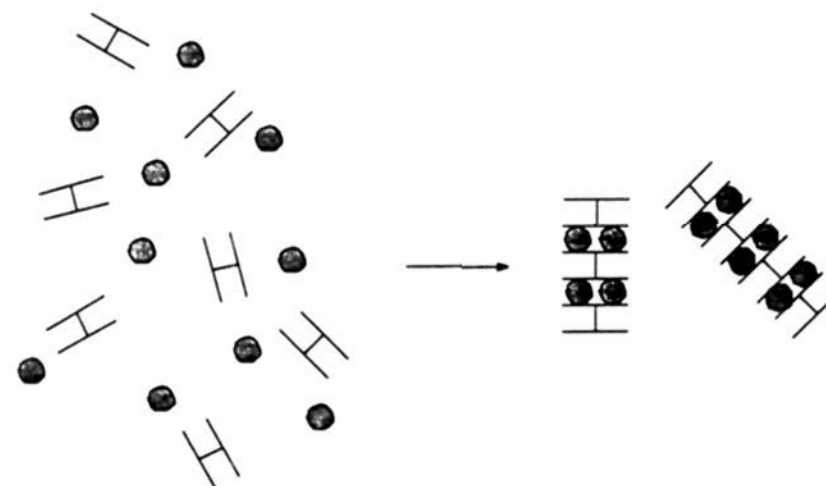


Figure 12. Aggregation induced by the formation of sandwich complexes between alkali cations and crown ether-substituted phthalocyanines. Aggregation occurs above a given critical concentration.

between the redox properties of the lutetium complex subunit and the binding of alkali ions by the crown ether moieties has been demonstrated. In chloroformic solutions, large cations lead to sandwich complexes. The titration curves indicate that the complexation of the first cation facilitates the binding of the second, third, and fourth cations, therefore demonstrating an allosteric effect. For the couple $[(18\text{-C-}6)_4\text{Pc}]_2\text{Lu/Rb}^+$, a sigmoidal titration curve has been observed. It can be interpreted by assuming two nonlinear processes: (i) the previous allosteric effect for the ion complexation at each elementary step of the formation of the aggregate and (ii) the presence of high molecular weight derivatives only above some critical concentration.

It is now necessary to integrate these ligands into networks. Work is in progress to functionalize the grid of field transistors in order to obtain such systems.

Experimental Section

(i) **Synthesis.** 4,5-Dicyanobenzo-15-crown-5 and 4,5-dicyanobenzo-18-crown-6 have been synthesized according to previously reported

procedures.¹²⁻¹⁴ The diether **7** was prepared by reacting pyrocatechol with 1-chloro-8-methoxy-3,6-dioxaoctane in the presence of NaOH (yield 64%).^{43,44}

All chemicals and solvents were reagent grade and were employed without further purification except for the solvents used for recrystallization: CH₂Cl₂, *n*-pentane, and *n*-heptane. The *n*-pentane and *n*-heptane solvents were distilled onto CaCl₂ and Na, respectively. The purity of **8** and **9** was checked by a gas chromatography-mass spectrometry (GCMS) apparatus (Hewlett-Packard). IR spectra were recorded on a Perkin-Elmer FTIR spectrometer. UV-visible absorption spectra were measured with a Kontron UVIKON 360 spectrophotometer. Elemental analyses were performed at ICS-Strasbourg. FAB and field desorption mass spectrometry measurements were carried out at the "Service de spectrométrie de masse de Strasbourg" and the "Institut für organische Chemie II" at Tübingen.

Bis[4,5,4',5',4'',5'',4''',5''']-tetrakis(1,4,7,10,13-pentaoxatridecamethylene)phthalocyanine]lutetium(III) (1). A round-bottomed flask fitted with a condenser was degassed and flame-dried under dry argon. The flask was charged under argon with the dinitrile derivative **5** (1 g, 3.14 mmol), Lu(OAc)₃·3H₂O (138 mg, 0.392 mmol), 1,8-diazabicyclo[5.4.0]-undec-7-ene (DBU) (234 μL, 1.57 mmol), and 7 mL of hexan-1-ol; the mixture was refluxed for 20 h. The reaction mixture was filtered on Celite after cooling, and the dark green precipitate was washed with warm *n*-heptane. Purification was achieved by (i) column chromatography over neutral alumina (elution gradient CHCl₃:EtOH from 100:0 to 97:3 v:v) and (ii) preparative thin-layer chromatography (neutral alumina, 2-mm thickness; eluent, CHCl₃:EtOH, 96:4 (v:v); R_f = 0.5). The compound was finally recrystallized from a mixture CH₂Cl₂:*n*-pentane (10:3 v:v) to afford a green powder in 19% yield (200 mg).

Anal. Calcd for C₁₂₈H₁₄₄O₄₀N₁₆Lu·4H₂O [*M*_w = 2721 + 4(18)]: C, 55.03; H, 5.48; N, 8.02; Lu, 6.26. Found: C, 55.24; H, 5.33; N, 7.8; Lu, 6.15. Mass spectrometry (FAB) *m/z*: 2721 (M⁺). IR (KBr): 3071, 2860, 1602, 1498, 1450, 1400, 1357, 1323, 1276, 1127, 1102, 1056, 934, 855, 811, 756 cm⁻¹. UV-visible (CHCl₃): ε₂₉₀ 102 000, ε₃₆₇ 132 000, ε₄₇₆ 38 400, ε₆₀₂ 30 200, ε₆₆₆ 165 000. Near-IR (CHCl₃): ε₉₁₀ 6000, ε₁₃₉₀ 16 000.

Bis[4,5,4',5',4'',5'',4''',5''']-tetrakis(1,4,7,10,13,16-hexaoxahexadecamethylene)phthalocyanine]lutetium(III) (2). The phthalonitrile **6** (1 g, 2.76 mmol) was reacted as described for **1**. Purification necessitated two successive preparative thin-layer chromatographies (neutral alumina, 2-mm thickness; eluent, CHCl₃:EtOH, 96:4 (v:v); R_f = 0.5). A final purification was achieved by recrystallization from a mixture of (CH₂-Cl₂):*n*-heptane (1:1 v:v) to afford dark green needles in 7% yield (70 mg).

Anal. Calcd for C₁₄₄H₁₇₆O₄₈N₁₆Lu·4H₂O [*M*_w = 3074 + 4(18)]: C, 54.92; H, 5.89; N, 7.12; Lu, 5.56. Found: C, 54.84; H, 5.77; N, 7.03; Lu, 5.57. Mass spectrometry (FAB) *m/z*: 3074 (M⁺), 1537 (M⁺/2). IR (KBr): 2871, 1602, 1500, 1452, 1387, 1353, 1325, 1275, 1197, 1117, 1054, 941, 859, 811, 756 cm⁻¹. UV-visible (CHCl₃): ε₂₉₁ 100 000, ε₃₆₈ 136 000, ε₄₇₆ 38 000, ε₆₀₂ 29 500, ε₆₆₆ 173 000.

1,2-Bis(9-methoxy-1,4,7-trioxanonyl)-4,5-dibromobenzene (8). In a 250-mL three-necked flask containing 150 mL of CH₂Cl₂, 10 g (0.025 mol) of compound **7**, 210 mg of iron powder, and iodine in catalytic amount was added dropwise a solution of 8.38 g (0.053 mol) of bromine in 50 mL of CH₂Cl₂ in 2 h at 0 °C. After the mixture was warmed to ambient temperature, stirring was continued overnight (20 h). The mixture was treated with an aqueous solution of sodium hyposulfite and sodium hydroxide until decoloration. The organic layer was washed with distilled water (three times), dried (MgSO₄), and evaporated under reduced pressure. The crude oil obtained was purified by column chromatography on silica gel (eluent, CH₂Cl₂:Et₂O, 50:50), yielding 8.5 g of a yellow oil (62%).

Anal. Calcd for C₂₀H₃₂O₈Br₂ (*M*_w = 560): C, 42.88; H, 5.76; Br, 28.52. Found: C, 42.59; H, 5.84; Br, 28.81. Mass spectrometry (GCMS) *m/z*: 562, 560, 558 (M⁺), 147 ((C₂H₄O)₃Me), 103 ((C₂H₄O)₂Me), 59 (C₂H₄OMe). ¹H NMR (300 MHz, CDCl₃): δ 3.37 (s, 6H, OCH₃), 3.54 (t, 4H, *J* = 4.48 Hz), 3.65 (m, 8H), 3.84 (t, 4H, *J* = 4.98 Hz), 3.84 (t, 4H, *J* = 4.88 Hz), 4.13 (t, 4H, *J* = 4.88 Hz), 7.14 (s, 2H, aromatic protons). ¹³C NMR (75 MHz, CDCl₃): 58.98, 69.27, 69.54, 70.53, 70.65, 70.85, 71.89, 115.25, 119.05, 148.85. IR (KBr): 2876, 1582, 1497, 1452, 1351, 1328, 1296, 1251, 1200, 1110, 1052, 948, 853, 651 cm⁻¹.

1,2-Bis(9-methoxy-1,4,7-trioxanonyl)-4,5-dicyanobenzene (9). A mixture of 8.5 g (0.015 mol) of **8**, 4.08 g (0.046 mol) of CuCN, and 125 mL

of freshly distilled DMF was refluxed under nitrogen overnight (16 h). After cooling of the solution and removal of the solvent, the crude product, dissolved in dichloromethane, was treated with 200 mL of aqueous NH₄OH (25%), and air was passed through the solution for 24 h. The aqueous solution became dark blue. A similar treatment was made with 200 mL of ethylenediamine (25%). The organic layer was washed with distilled water, dried (MgSO₄), filtered, and concentrated under reduced pressure. The green-brownish oil was chromatographed on silica gel (elution gradient, CH₂Cl₂:MeOH from 100:0 to 97:3), and an orange oil was obtained in a 70% yield (5 g).

Anal. Calcd for C₂₂H₃₂O₈N₂ (*M*_w = 452): C, 58.39; H, 7.13; N, 6.19. Found: C, 57.83; H, 7.27; N, 5.86. Mass spectrometry (GCMS) *m/z*: 452 (M⁺), 186 (M⁺ - ((C₂H₄O)₃Me) - ((C₂H₄O)₂Me)), 171 (M⁺ - ((C₂H₄O)₃Me) - (CH₂O(C₂H₄O)Me)), 147 ((C₂H₄O)₃Me), 103 ((C₂H₄O)₂Me), 89 (CH₂O(C₂H₄O)Me), 59 (C₂H₄OMe). ¹H NMR (300 MHz, CDCl₃): δ 3.37 (s, 6H, OCH₃), 3.55 (t, 4H, *J* = 4.44 Hz), 3.65 (m, 8H), 3.74 (t, 4H, *J* = 4.7 Hz), 3.91 (t, 4H, *J* = 4.59 Hz), 4.27 (t, 4H, *J* = 4.6 Hz), 7.30 (s, 2H, aromatic protons). ¹³C NMR (75 MHz, CDCl₃): δ 58.26, 68.65, 68.85, 69.82, 69.94, 70.26, 71.23, 107.92, 115.32, 116.45, 151.74. IR (KBr): 2879, 2230, 1590, 1564, 1519, 1453, 1408, 1352, 1290, 1230, 1215, 1200, 1103, 1042, 949, 891, 852 cm⁻¹.

Bis[4,5,4',5',4'',5'',4''',5''']-octakis(9-methoxy-1,4,7-trioxanonyl)phthalocyanine]lutetium(III) (3). This compound was synthesized from **9** (1 g, 2.08 mmol) as described for **1**. After filtration on Celite, solids were put into the thimble of a Soxhlet apparatus and extracted with *n*-heptane for 3 days in order to remove organic materials. Roughly purified phthalocyanines were recovered by extraction with chloroform. Two successive preparative thin-layer chromatographies (neutral alumina, 2-mm thickness; eluent, CHCl₃:ethyl acetate:propan-2-ol, 60:37:3 (v:v v); R_f = 0.5) and precipitation from a CH₂Cl₂:*n*-heptane (2:5 v:v) mixture led to 120 mg (yield, 11%) of a dark green paste.

Anal. Calcd for C₁₇₆H₂₅₆O₆₄N₁₆Lu (*M*_w = 3795): C, 55.70; H, 6.79; N, 5.91; Lu, 4.61. Found: C, 55.28; H, 6.88; N, 5.76; Lu, 4.44. Mass spectrometry (field desorption) *m/z*: 3797 (M⁺), 1908 ((M⁺ + 18)/2). IR (KBr): 2873, 1599, 1560, 1500, 1452, 1389, 1352, 1322, 1278, 1204, 1108, 1062, 938, 858, 812, 757 cm⁻¹. UV-visible (CH₂Cl₂): ε₂₉₁ 112 000, ε₃₆₇ 152 000, ε₄₇₅ 43 000, ε₅₉₉ 32 000, ε₆₆₂ 197 000.

[4,5,4',5',4'',5'',4''',5''']-Octakis(9-methoxy-1,4,7-trioxanonyl)phthalocyanine[4,5,4',5',4'',5'',4''',5''']-tetrakis(1,4,7,10,13-pentaoxatridecamethylene)phthalocyanine]lutetium(III) (4). A mixture of (15-C-5)₄PcLu(OAc)(2H₂O) (90 mg, 0.06 mmol), compound **7** (216 mg, 0.48 mmol), and DBU (36 μL, 0.24 mmol) in hexan-1-ol (5 mL) was refluxed overnight. After the mixture was cooled, the crude product was filtered on Celite, and the precipitate was washed with warm *n*-heptane and *n*-heptane: ethyl acetate mixture (4:1 v:v). The remaining materials were extracted with CH₂Cl₂, and purification was achieved by two successive preparative thin-layer chromatographies (neutral alumina, 2-mm thickness; eluent, CHCl₃:EtOH, 96:4 (v:v); R_f = 0.65). The product was finally precipitated from a CH₂Cl₂:*n*-heptane mixture (1:2 v:v) to afford a green paste in 7.5% yield (15 mg).

Anal. Calcd for C₁₅₂H₂₀₀O₅₂N₁₆Lu (*M*_w = 3258): C, 56.03; H, 6.19; N, 6.88; Lu, 5.37. Found: C, 55.49; H, 6.10; N, 6.63; Lu, 5.06. Mass spectrometry (field desorption) *m/z*: 3258 (M⁺). IR (KBr): 2924, 2865, 1600, 1499, 1451, 1361, 1322, 1278, 1127, 1204, 1108, 1081, 1059, 935, 858, 810, 756 cm⁻¹.

Compounds **1** and **2** are soluble in CHCl₃ and CH₂Cl₂, whereas derivatives **3** and **4** are soluble in all organic solvents (CHCl₃, CH₂Cl₂, methanol, acetone, ethyl acetate, ether, DMF, etc.), slightly soluble in water, and insoluble in alkanes.

(ii) **Measurements.** NMR experiments were carried out using a Bruker AM 300 spectrometer working at 300.13 (1H) and 75 MHz (13C) under broad-band proton decoupling. Chemical shifts were referenced to internal TMS and CDCl₃ (77 ppm/TMS). Reductions were performed by dissolving under argon the phthalocyanine derivative (7 mg) in DMF-*d*₇ (0.5 mL) in the presence of LiBH₄ (2 mg). Oxidation was achieved by adding bromine in CDCl₃ (20 μL, 0.58 M) to a solution of phthalocyanine derivative (7 mg) in CDCl₃:CD₃OD, 5:1 (0.5 mL).

¹H NMR chemical shifts for ligands **1-4** in CDCl₃ are given in Table 5.

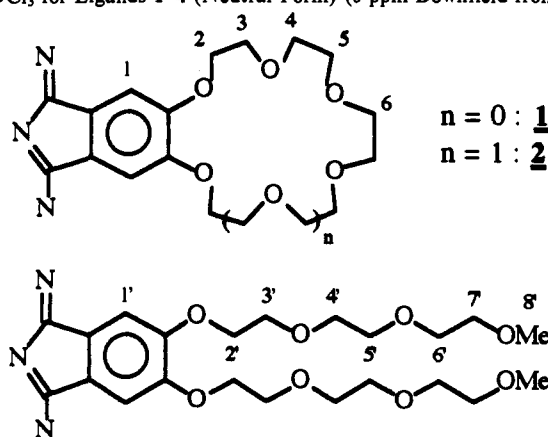
The ¹³C assignments for crown ether-substituted molecules were obtained by analogy with those previously made for benzo-18-crown-6.^{28,29} The work of Ribeiro and Denis⁴⁵ on alkylated poly(oxyethylene) was used for the assignments of **3**.

¹³C NMR chemical shifts are given in Table 6.

(43) Chaput, G.; Jeminet, G.; Juillard, J. *Can. J. Chem.* **1975**, *53*, 2240.

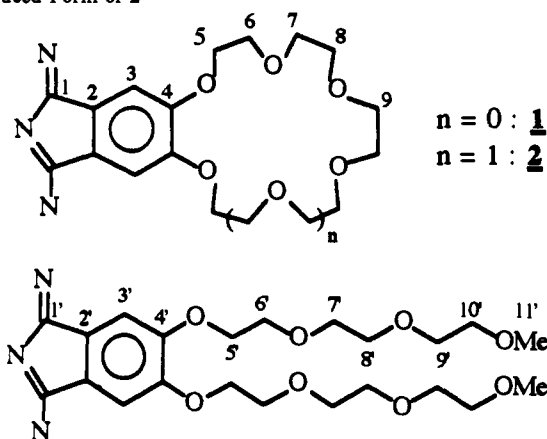
(44) Stolwijk, T. B.; Vos, L. C.; Sudhölter, E. J. R.; Reinhoudt, D. N. *Recl. Trav. Chim. Pays-Bas* **1989**, *108*, 103.

(45) Ribeiro, A. A.; Denis, A. E. *J. Phys. Chem.* **1977**, *81*, 957.

Table 5. ^1H NMR Chemical Shifts in CDCl_3 for Ligands 1–4 (Neutral Form) (δ ppm Downfield from TMS)^a

1		2		3		4	
δ	atom	δ	atom	δ	atom	δ	atom
4.10 (32H)	3	4.19 (32H)	3	4.21 (32H)	3'	4.18 (32H)	3, 3'
3.99 (32H)	4	3.93 (32H)	4	3.95 (32H)	4'		
						3.91 (48H)	4, 4', 5
3.89 (32H)	5	3.84 (32H)	5				
		3.80 (32H)	6				
				3.79 (32H)	5'	3.80 (16H)	5'
				3.70 (32H)	6'	3.71 (16H)	6'
				3.58 (32H)	7'	3.59 (16H)	7'
				3.38 (48H)	8'	3.39 (24H)	8'

^a The corresponding number of H atoms is indicated in parentheses.

Table 6. ^{13}C NMR Chemical Shifts (δ ppm Downfield from TMS) and Assignments for the Neutral Forms of 2, 3, and 4 and the Reduced Form of 2

2		3 ^a		4 ^a	
neutral form ^a	reduced form ^b	δ	atom	δ	atom
	159.0				
	150.0				
	131.6				
	105.3				
		72.00	10'	72.01	10'
		71.15	9'	71.12	9'
71.0	9			71.02	8
70.7	8	70.82	8'	70.84	8'
70.6	7	70.62	7'	70.63	7'
69.4	6			70.20	7
		69.5	6	69.92	6'
		69.1	5	69.43	6
				59.03	11'
				59.06	11'

^a CDCl_3 . ^b DMF.

Alkali Metal Picrate Extraction. This method is based on the extraction of aqueous solutions of metal picrate salts (5×10^{-3} M) by chloroformic solution of ionophore ($[\text{CR}_0] = 5 \times 10^{-3}$ M crown ether, i.e., 6.25×10^{-4}

M 1 or 2) at 25 °C. Subsequently the picrate concentrations were obtained by UV-visible measurements at 375 nm in CH_3CN .

Because of the high absorbances of the phthalocyanines in the 375-nm region and of the small extraction values for 1 (prohibiting reproducible direct measurements of the picrate concentration in the aqueous layer), a modified experimental procedure was developed. After extraction, the organic solution was filtered over cotton wool and reextracted with pure distilled water (2×1 mL) in order to release the picrate salt. UV-visible measurements on the aqueous solution after dilution with CH_3CN led to the concentration of extracted picrate $[\text{M}^+\text{Pic}^-]_{\text{ex}}$. Direct measurements on 2 from the aqueous layer have confirmed the reliability of our procedure.

All volumes used for extraction were 1 mL. The extinction coefficients, ϵ , for alkali metal picrate were Li^+ , 17 300; Na^+ , K^+ , 17 200; Rb^+ , Cs^+ , 17 800 (determined in the range 0 – 10^{-4} M). The K_p values were those given by the literature.³² Then,

$$[\text{M}^+\text{Pic}^-]_{\text{ex}} = [\text{M}^+\text{LPic}^-]_{\text{org}} + [\text{M}^+\text{Pic}^-]_{\text{org}}$$

$$[\text{CR}_0] = [\text{CR}]_{\text{org}} + [\text{M}^+\text{LPic}^-]_{\text{org}}$$

$$[\text{M}_0] = [\text{M}^+]_{\text{aq}} + [\text{M}^+\text{Pic}^-]_{\text{aq}} + [\text{M}^+\text{LPic}^-]_{\text{org}}$$

Assuming $[\text{M}^+\text{LPic}^-]_{\text{org}} \gg [\text{M}^+\text{Pic}^-]_{\text{org}}$ and according to eq 2:

$$[\text{CR}]_{\text{org}} = [\text{CR}_0] - [\text{M}^+\text{LPic}^-]_{\text{org}} = [\text{CR}_0](1 - R)$$

$$[\text{M}^+]_{\text{aq}} = [\text{Pic}^-]_{\text{aq}} = [\text{M}_0] - [\text{M}^+\text{LPic}^-]_{\text{org}} = [\text{M}_0] - R[\text{CR}_0]$$

$$[\text{M}^+\text{Pic}^-]_{\text{org}} = K_p[\text{M}^+]_{\text{aq}}[\text{Pic}^-]_{\text{aq}}$$

The extracted ratio R , the association constant K_a , and the complexation free enthalpy ΔG_0 are given by:

$$R = \frac{[\text{M}^+\text{pic}^-]_{\text{ex}}}{[\text{CR}_0]}$$

$$K_a = \frac{R}{K_p(1 - R)([\text{M}_0] - R[\text{CR}_0])}$$

$$\Delta G_0 = -RT \ln K_a$$

with

K_p	partition constant
$[CR_0] = 8[L_0]$	initial crown ether concentration in the organic layer
$[M_0]$	initial alkali metal picrate in the aqueous layer

Absorption Spectroscopy. All measurements were performed in 1-cm quartz cells. The reduced (respectively oxidized) form was prepared by adding 0.2 mL of N_2H_4/H_2O (respectively 0.1 mL DDQ/ CH_2Cl_2 , 2 mg/1 mL) to 2 mL of a chloroformic solution of **1** (10^{-5} M).

Aggregation studies were carried out by recording the changes of the absorption spectra resulting from addition of alkali metal picrate to 2 mL of a $CHCl_3$ solution (10^{-5} M) of **1**, **2**, or **4**. The picrate salts were dissolved in MeOH (2×10^{-3} M) and were added by portion with a microsyringe: 150 μ L were added in total. Using the following definitions,

l	cell length
$[L_0]$	initial concentration of the dye
$[L_1]$	concentration of free dye
$[L_2]$	concentration of dye in aggregates
A_1	absorbance of the monomeric species
ϵ_1	molar extinction coefficient of the monomeric species
A_2	absorbance of the aggregates (plateau value)
ϵ_2	molar extinction coefficient of the aggregates
A	observed absorbance

the apparent molar extinction coefficient is given by:

$$\frac{A_1 - A}{l[L_0]}$$

The following treatment was considered to obtain $[L_2]/[L_0] = f([M^+]/[L_0])$:

$$[L_0] = [L_1] + [L_2]$$

$$A = l(\epsilon_1[L_1] + \epsilon_2[L_2])$$

By combination of those equations, we easily calculated

$$[L_2] = \frac{A_1 - A}{l(\epsilon_1 - \epsilon_2)}$$

with

$$\epsilon_1 = \frac{A_1}{l[L_0]} \quad \epsilon_2 = \frac{A_2}{l[L_0]}$$

Acknowledgment. Mr. Revial, Mr. Plichon, Mr. Van Dorselaer, and Mr. Chassignard are thanked for helpful discussions and precious assistance.